Simulation of Non-Acoustic Combustion Instability in a Hybrid Rocket Motor[a]

Marvin Rocker
Fluid Physics and Dynamics Group
NASA/Marshall Space Flight Center
Huntsville, Alabama

ABSTRACT:

A transient model of a hybrid motor was formulated to study the cause and elimination of non-acoustic combustion instability. The transient model was used to simulate four key tests out of a series of seventeen hybrid motor tests conducted by Thiokol, Rocketdyne and Martin Marietta at NASA/Marshall Space Flight Center (NASA/MSFC). These tests were performed under the Hybrid Propulsion Technology for Launch Vehicle Boosters (HPTLVB) program. The first test resulted in stable combustion. The second test resulted in large-amplitude, 6.5 Hz chamber pressure oscillations that gradually damped away by the end of the test. The third test resulted in large-amplitude, 7.5 Hz chamber pressure oscillations that were sustained throughout the test. The seventh test resulted in the elimination of combustion instability with the installation of an orifice immediately upstream of the injector. The formulation and implementation of the model are the scope of this presentation.

The current model is an independent continuation of modeling presented previously by joint Thiokol-Rocketdyne collaborators Boardman, Hawkins, Wassom, and Claflin. The previous model simulated an unstable IR&D hybrid motor test performed by Thiokol. There was very good agreement between the model and the test data.

Like the previous model, the current model was developed using Matrix-x simulation software. However, the tests performed at NASA/MSFC under the HPTLVB program were actually simulated.

In the current model, the hybrid motor consisting of the liquid oxygen (LOX) injector, the multi-port solid fuel grain and the nozzle was simulated. Also, simulated in the model was the LOX feed system consisting of the tank, venturi, valve and feed lines. All components of the hybrid motor and LOX feed system are treated by a lumped-parameter approach.

Agreement between the results of the transient model and the actual test data was very good. This agreement between simulated and actual test data indicated that the combustion instability in the hybrid motor was due to two causes. The first cause was a LOX feed system of insufficient stiffness. The second cause was a LOX injector with an impedance or pressure drop that was too low to provide damping against the feed system oscillations. Also, it was discovered that testing with a new grain of solid fuel sustained the combustion instability. However, testing with a used grain of solid fuel caused the combustion instability to gradually decay.

INTRODUCTION:

Non-acoustic combustion instabilities are high-amplitude chamber pressure oscillations that have frequencies too low to be characterized as acoustic in nature. In hybrid motors, combustion instability of any frequency range may be initiated by one or all of four mechanisms[1]. The first mechanism is poor atomization from the injector in the head-end vaporization chamber. The second mechanism is chuffing of the solid fuel in the ports.

---

[a] Approved for public release, distribution is unlimited.

The third mechanism is the pressure-sensitivity of the combustion process, also in the fuel ports. The fourth mechanism is flow-induced oscillations caused by vortex shedding in the aft mixing chamber. A fifth mechanism of non-acoustic combustion instability, that is not intrinsic to the hybrid motor, is the hydrodynamic feed system coupling between the hybrid motor and the LOX feed system.

A series of seventeen subscale hybrid motor tests were conducted by Thiokol, Rocketdyne and Martin Marietta at test stand 500 at NASA/Marshall Space Flight Center in Huntsville, Alabama. The hybrid motor during pre-test preparation and during hot-fire testing is illustrated in figures-1 and 2, respectively. These tests were conducted for the Hybrid Propulsion Technology for Launch Vehicle Boosters (HPTLVB) program[2], funded under contract NAS8-39942. The test objective was to investigate the effects of oxidizer pre-combustion and oxidizer distribution on the combustion stability of hybrid motors. The mainstage duration of these tests was about 10 seconds. During some of these tests, non-acoustic combustion instabilities were observed.

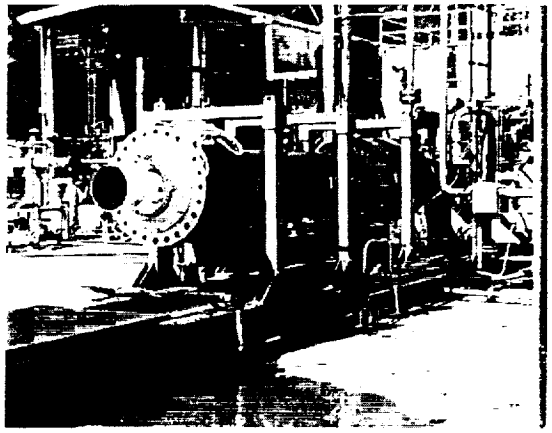

Figure-1: The 24-inch hybrid motor prior to testing.

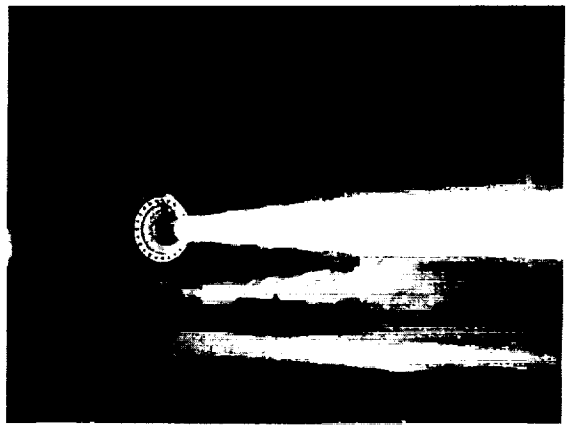

Figure-2: The 24-inch hybrid motor during hot-fire testing.

DESCRIPTION OF THE HYBRID TEST SYSTEM:

The test system consists of the hybrid motor and the LOX feed system.

The sketch of the hybrid motor is presented in figure-3. The hybrid motor has a case diameter of 24 inches (61 cm). At the head end of the hybrid motor is the vaporization chamber. The vaporization chamber is lined with solid fuel, which when burned vaporizes the LOX. The vaporization chamber had optional solid fuel fins. These fins extended radially from the walls to the center of the chamber. These fins enhanced LOX vaporization. Within the vaporization chamber is the LOX injector. Two injectors were used in the test series. The first injector was used in the Large Subscale Solid Rocket Combustion Simulator (LSSRCS) test series. The second injector was used in the Joint Industry Research And Development (JIRAD) test series. The design of both of these injectors will be presented later. Downstream of the vaporization chamber is the solid fuel grain. The solid fuel grain is 108 inches (274 cm) long and is consists of HTPB-based fuel. The solid fuel grain has six outer ports and a center port arranged in a wagon-wheel cross-section. Downstream of the solid fuel grain at is the mixing chamber. Downstream of the mixing chamber is the nozzle.

The schematic for the LOX feed system is presented in figure-4. The LOX feed system consists of a 3000 gallon (11,356 liters) LOX tank, the cavitating venturi and the valve, respectively. Between these components is a total of 255 feet (78 m) of 3-inch (7.6 cm) diameter feedline.

TEST RESULTS:

The results of the first seven tests are presented as follows.

For test-1, the motor was tested with the LSSRCS injector, without the solid fuel fins in the vaporization chamber. The LOX flow rate was 10 lbm/sec (4.5 kg/sec) with an injector pressure drop of about 44% of chamber pressure. A chamber pressure of 470 psi (3.2 MPa) was achieved. The test was stable, with no oscillations in the chamber pressure.

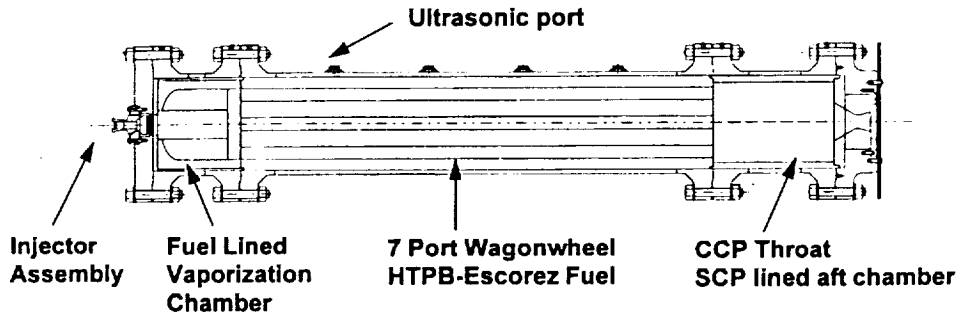

Figure-3: The 24-inch hybrid motor.

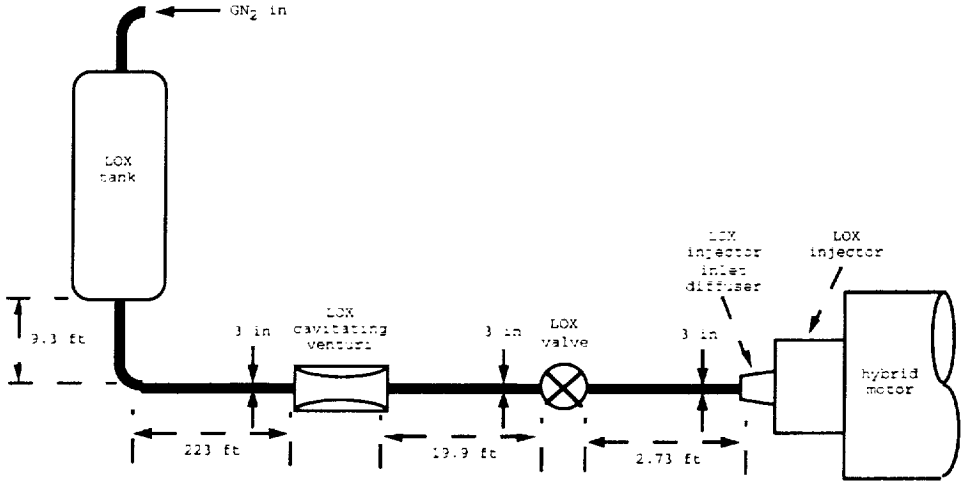

Figure-4: The LOX feed system for the 24-inch hybrid motor tests.

For test-2, the motor was tested unaltered from test-1 with the exception of the injector. The test was performed with the JIRAD injector. The LOX flow rate was 20 lbm/sec (9.1 kg/sec) with an injector pressure drop of 11% of chamber pressure. A chamber pressure of 440 psi (3.0 MPa) was achieved. Unlike test-1, test-2 was unstable with large amplitude, 6.5 Hz oscillations in chamber pressure that decayed just before the end of the test. The maximum amplitude of the oscillations was about 20% (peak to peak) of chamber pressure.

For test-3, the motor was tested with a new solid fuel grain, with solid fuel fins in the vaporization chamber and with the JIRAD injector. The LOX flow rate was 20 lbm/sec (9.1 kg/sec) with an injector pressure drop of 14% of chamber pressure. A chamber pressure of 420 psi (2.9 MPa) was achieved. Test-3 was unstable with large amplitude 7.5 Hz oscillations in chamber pressure that were sustained throughout the test. The amplitude of the oscillations was about 25% (peak to peak) of chamber pressure.

For test-4, the motor was tested with a used solid fuel grain, a new vaporization chamber with solid fuel fins and with the JIRAD injector. The motor was accidently tested with two venturis flowing LOX in parallel (not shown in figure-4). The resulting LOX flow rate was 40 lbm/sec (18.2 kg/sec) with an injector pressure drop of 29% of chamber pressure. A chamber pressure of 850 psi (5.8 MPa) was achieved, initially. The chamber pressure decreased linearly to 600 psi (4.1 MPa) by the end of the test. Test-4 was stable with small amplitude 5 Hz oscillations in chamber pressure.

Test-5 was essentially a repeat of test-3. For this test, the motor was tested with a new solid fuel grain, with solid fuel fins in the vaporization chamber and with the JIRAD injector. The LOX flow rate was 20 lbm/sec (9.1 kg/sec) with an injector pressure drop of 13% of chamber pressure. A chamber pressure of 450 psi (3.1 MPa) was achieved. Test-5 was unstable with large amplitude 6.5 Hz oscillations in chamber pressure that were sustained throughout the test. The amplitude of the oscillations was about 25% (peak to peak) of chamber pressure.

Test-6 was a repeat of test-4. In test-6, the motor was tested with a used solid fuel grain, a new vaporization chamber with solid fuel fins and a JIRAD injector. For the test, both valves (not shown in figure-4), which enabled the selection of two different venturis, were simultaneously opened. The resulting LOX flow rate was 40 lbm/sec (18.2 kg/sec) with an injector pressure drop of 29% of chamber pressure. A chamber pressure of 850 psi (5.8 MPa) was achieved, initially. The chamber pressure decreased linearly to 600 psi (4.1 MPa) by the end of the test. Test-6 had marginally stable oscillations in chamber pressure. The amplitude of these oscillations were about 10% (peak to peak) of chamber pressure.

Test-7 was the second repeat of test-3. For this test, the motor was tested with a new solid fuel grain, with solid fuel fins in the used vaporization chamber and with the JIRAD injector. Also, this test was performed with an orifice immediately upstream of the injector. This orifice was intended to decouple the injector and motor from the hydrodynamics of the feed system. The LOX flow rate was 20 lbm/sec (9.1 kg/sec) with an injector pressure drop of about 10% of chamber pressure. A chamber pressure of 450 psi (3.1 MPa) was achieved. Test-7 was stable with small amplitude oscillations in chamber pressure that were sustained throughout the test. The amplitude of the oscillations was about 6% (peak to peak) of chamber pressure.

The conclusion of the test series was that the 24-inch (61 cm) hybrid motors were producing large amplitude, 6.5 Hz oscillations in chamber pressure that were too low in frequency to be acoustic in nature. A further study of the test data indicated that coupling between the combustion chamber and the feed system hydrodynamics was occurring. This theory was verified in test-7 by decoupling the chamber from the feed system with an orifice immediately upstream of the injector. This decoupling resulted in a reduction in the amplitude of chamber pressure oscillations to an acceptable level. Similar results were obtained in the subsequent tests by replacing the orifice with an additional cavitating venturi immediately upstream of the injector.

INITIAL MODELING EFFORT:

To investigate the non-acoustic combustion instabilities that were exhibited during the test series, joint Thiokol-Rocketdyne collaborators, Boardman, Hawkins, Wassom and Claflin formulated a non-linear transient model[3,4] of the LOX feed system and the hybrid motor.

The approach consisted of modeling the LOX feed system and the hybrid motor combustion chamber coupled through the LOX injector. The features that were modeled in the LOX feed system were LOX compressibility, feedline volume, GOX volume and unsteady mass conservation. The LOX injector was modeled by Bernoulli's equation. The features that were modeled in the hybrid motor combustion chamber were port volume, fuel

regression, gas properties, unsteady mass conservation, unsteady energy conservation, gas equation of state and distributed vaporization.

The transient model was implemented with Matrix-x system simulation software. Matrix-x facilitates the on-screen, graphical construction of a model of any dynamic system that can be represented by a system of non-linear ordinary differential equations. A model of a dynamic system is constructed by assembling together block-elements that represents integrators, gains, adders, multipliers, limiters, etc. Entire subsystems may be assembled in this fashion to form a model of a complex dynamic system.

The model was verified by simulating a 24-inch (61 cm) hybrid motor test performed independently by Thiokol. This test exhibited non-acoustic combustion instabilities similar to those observed in tests-2, 3 and 5 at NASA/MSFC. In the model, a "soft" LOX feed system was assumed. A "soft" feed system contains highly compressible LOX. The simulation had very good agreement with the test data. A "stiff" feed system contains LOX that is not as compressible as LOX in a "soft" feed system. Clearly, LOX compressibility in the feed system seems to be a factor in determining the non-acoustic combustion stability of a hybrid motor.

Funding was exhausted before simulation of the test series conducted at NASA/MSFC could be performed.

CURRENT MODELING EFFORT:

To investigate the non-acoustic combustion instabilities observed in tests-2, 3 and 5, an independent model was developed at NASA/MSFC. The current model is based on a lumped-parameter representation of conservation of mass and energy in the combustion chamber and conservation of mass and momentum in the injector, the feed system components and the tank. Also, two out of four of the hybrid combustion instability mechanisms are represented in the current model. The first instability mechanism is atomization/vaporization, which is modeled by a time lag. The second instability mechanism is the pressure sensitivity of the regression rate, whose model is based on the best curve fit of the 24-inch (61 cm) hybrid tests conducted under the Hybrid Propulsion Development Program[5] (HPDP). This model closely matches the fifth out a collection of nine models presented in the literature[6]. The third instability mechanism is chuffing, is not explicitly modeled. The fourth instability mechanism is vortex shedding, which is not represented in the current model.

LOX INJECTOR DESIGNS:

The LOX injector in the vaporization chamber of the hybrid motor is illustrated in figure-5. The parameters of the LOX injector model are obtained from the designs of the LSSRCS and JIRAD injectors presented as follows.

LSSRCS LOX INJECTOR DESIGN:

The LSSRCS LOX injector design is presented in figures-6 and 7. The LSSRCS LOX injector is a simple impingement injector with 634 orifices. These orifices are 0.022 inches (0.559 mm) in diameter in a faceplate that is 0.125 inches (3.175mm) thick and 4.745 inches (12.052 cm) diameter. The orifices are arranged into 317 doublets, each with an impingement angle 60°. The total LOX dome volume, including the volume of the downcomers, is 24 cubic inches(393 cubic cm).

JIRAD LOX INJECTOR DESIGN:

The JIRAD LOX injector and its faceplate design is presented in figures-8 and 9, respectively. The JIRAD LOX injector is a complex impingement injector with 332 orifices. The orifices are divided into 157 elements of 6 different element types, A-F.

Type-A is a quadlet with an orifice diameter of 0.080 inches (2.032 mm) and a doublet impingement angle of 60°. There are 21 type-A elements that provide the primary portion of the core LOX flow. Type-B is doublet with an orifice diameter of 0.100 inches (2.540 mm) and an impingement angle of 60°. There are 12 type-B elements that provide the secondary portion of the core LOX flow.

Type-C is a doublet with an orifice diameter of 0.033 inches (0.838 mm) and an impingement angle of 60°. There are 88 type-C elements that surrounds all of the type-A, B, D and E elements. Type-D is an atypical doublet with an orifice diameter of 0.064 inches (1.626 mm) and an impingement angle of 36°. One of the two type-D orifices is directed axially, the other is angled. There are 8 type-D elements near the periphery of the injector face.

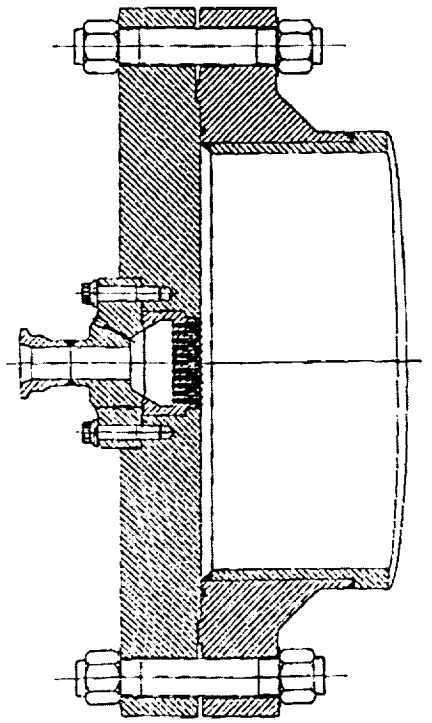

Figure-5: The LOX injector in the forward vaporization chamber.

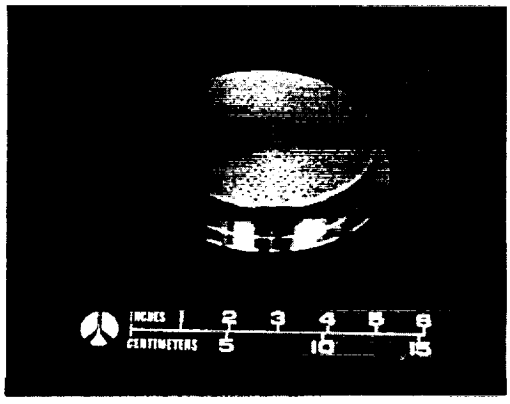

Figure-6: The LSSRCS LOX injector.

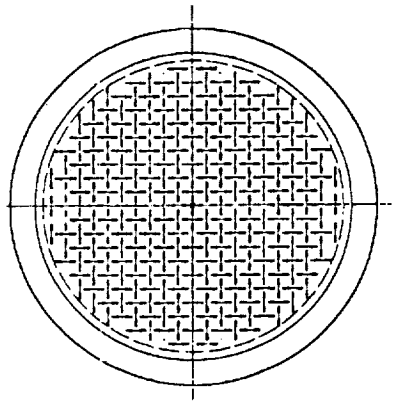

Figure-7: LSSCRS LOX injector faceplate design.

Type-E is a doublet with an orifice diameter of 0.080 inches (2.032 mm) and an impingement angle of 60°. There are 4 type-E elements located at each of the 4 corners of the pattern of type-A elements. The type-D and E elements make up the remainder of the LOX core flow. Type-F is a single orificed element with a diameter of 0.033 inches (0.838 mm) and angled outboard 30°. There are 24 type-F elements at the extreme periphery of the injector face.

MODELING OF JIRAD INJECTOR HYDRAULICS CONSTANTS:

Due the dissimilar orifice diameters, an average hydraulic diameter for the 332 orifices has been determined to be about 0.064 inches (1.626 mm). The total LOX dome volume, including the volume of the downcomers, is 17 cubic inches (279 cubic cm).

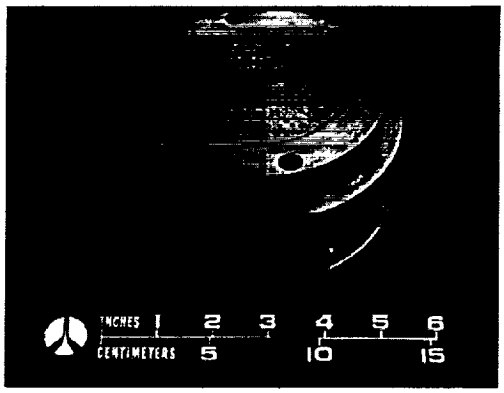

Figure-8: The JIRAD LOX injector.

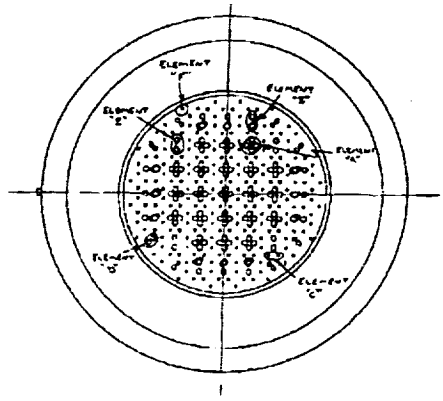

Figure-9: JIRAD LOX injector faceplate design.

MODELING OF VAPORIZATION/COMBUSTION TIME LAGS:

To determine the time lags for the LSSCRS and JIRAD injectors, a vaporization length of 128.5 inches (326.4 cm) is assumed. This is the combined length of the vaporization chamber and any one of the 7 ports that a LOX droplet will travel before being completely vaporized. From test-1 conditions and from the LSSCRS injector design, an injection velocity about 81 ft/sec (25 m/sec) has been determined. Therefore, the resulting time lag for test-1 is 0.13 seconds. From test-2 conditions and from the JIRAD injector design, an injection velocity about 45 ft/sec (14 m/sec) has been determined. Therefore, the resulting time lag for tests-2, 3, and 7 is 0.24 seconds.

MODELING OF PROPORTIONS OF LOX VAPORIZED IN THE COMBUSTION CHAMBER:

About 16% of the LOX flow rate is assumed to vaporize instantly in the vaporization chamber. The remaining 84% of the LOX flow rate is assumed to vaporize later in the ports. These percentages are based on the initial portions of solid fuel surface area in the ports and in the vaporization chamber.

RESULTS OF THE TEST-2 SIMULATION:

The actual and simulated test data for test-2 are presented in figures-10 and 11, respectively. Recall that test-2 was performed with the same fuel grain used in test-1, with a LOX flow rate of 20 lbm/sec (9.1 kg/sec), and with the low-impedance JIRAD injector with a pressure drop of 11%. The pressures being presented in both figures correspond to the upstream venturi pressure, the injection pressure, and the chamber pressure. There is a very good qualitative match between the actual and simulated test data. The chamber pressure

oscillations were initially at 20% of mean chamber pressure in amplitude and decayed gradually by the end of the test.

The chamber pressure oscillations in the actual test data were reported to have a frequency of about 6.5 Hz. In figure-12, a frequency spectrum of the simulated chamber pressure is presented. There are peaks in the spectrum at 2.5 Hz, 6.4 Hz, and 10.4 Hz. The peak at 2.5 Hz is primary in spectral intensity and corresponds to the "fill/flush" frequency. The peak at 6.4 Hz is slightly secondary in spectral intensity and corresponds to the non-acoustic combustion instability associated with the LOX feedline between the valve and the injector. The peak at 10.4 Hz is a distant third in spectral intensity and does not corresponds to any known cause.

Test-2 was simulated first since it was the first unstable test. The first few attempts at simulating test-2 resulted in non-oscillatory pressures in the combustion chamber and feedsystem downstream of the venturi. However, upstream of the venturi, the feedsystem pressure was oscillatory due to the "water hammer" effect. It was also noticed that, according to figure-4, the feedline volume upstream of the venturi was enormous. If the oscillations in feedsystem pressure was caused by a large feedline volume, then to cause oscillations in feedsystem pressure downstream of the venturi, the feedline volume downstream of the venturi had to be increased. Therefore, the feedline volume downstream of the venturi, between the valve and injector was increased 14.17 times the actual value. This increase was equivalent to the actual LOX compressibility being 14.17 times the compressibility as it was modeled. The large compressibility in this portion of feedline suggests the presence of trapped gaseous oxygen (GOX). This increase resulted in pressure oscillations in the chamber and in the feedsystem downstream of the venturi. Furthermore, these oscillations were initially at 20% of mean chamber pressure in amplitude and decayed gradually by the end of the test.

Capacitance[7] is the product of the feedline volume and compressibility. Increasing either volume, compressibility, or both results in increased capacitance. Stiffness is the reciprical of capacitance. It was a small capacitance or a large stiffness that resulted in a "stiff" feedsystem, making oscillations in the feedsystem impossible. It was a large capacitance or a small stiffness that resulted in a "soft" feedsystem, making oscillations in the feedsystem possible.

RESULTS OF THE TEST-3 SIMULATION:

The actual and simulated test data for test-3 are presented in figures-13 and 14, respectively. Recall that test-3 was performed with a fresh fuel grain, with a LOX flow rate of 20 lbm/sec (9.1 kg/sec), and with the low-impedance JIRAD injector with a pressure drop of 14%. As in test-2, there is a very good qualitative match between the actual and simulated test data. The chamber pressure oscillations were initially at 25% of mean chamber pressure in amplitude and was sustained throughout the test.

The chamber pressure oscillations in the actual test data were reported to have a frequency of about 7.5 Hz. In figure-15, a frequency spectrum of the simulated chamber pressure is presented. As in figure-12 for test-2, there are peaks in the spectrum at 2.5 Hz, 6.4 Hz, and 10.4 Hz. The peak at 2.5 Hz is secondary in spectral intensity and corresponds to the "fill/flush" frequency. The peak at 6.4 Hz now domainates in spectral intensity and corresponds to the non-acoustic combustion instability associated with the LOX feedline between the valve and the injector. The dominance of the peak in spectral intensity at 6.4 Hz seems to be related to the fact that the oscillations in pressure are sustained in test-3. The peak at 10.4 Hz is a distant third in spectral intensity and still does not corresponds to any known cause.

Test-3 was simulated second for two reasons. First, since test-3 was the second unstable test. Second, since the only difference between tests-2 and 3 was that while test-2 was performed with a used fuel grain, test-3 was performed with a new fuel grain. The first

attempt at simulating test-3 resulted in non-oscillatory pressures in the combustion chamber and feedsystem downstream of the venturi. Therefore, like test-2, the feedline volume downstream of the venturi, between the valve and injector was increased 14.17 times the actual value. This increase was equivalent to the actual LOX compressibility being 14.17 times the compressibility as it was modeled. This increase resulted in pressure oscillations in the chamber and in the feedsystem downstream of the venturi. Furthermore, these oscillations were initially at 25% of mean chamber pressure in amplitude and was sustained throughout the test.

RESULTS OF THE TEST-1 SIMULATION:

The actual and simulated test data for test-1 are presented in figures-16 and 17, respectively. Recall that test-1 was performed with a fresh fuel grain, with a LOX flow rate of 10 lbm/sec (4.5 kg/sec), and with the high-impedance LSSRCS injector with a pressure drop of 44%. As in tests-2 and 3, there is a very good qualitative match between the actual and simulated test data. There were no chamber pressure oscillations throughout the test.

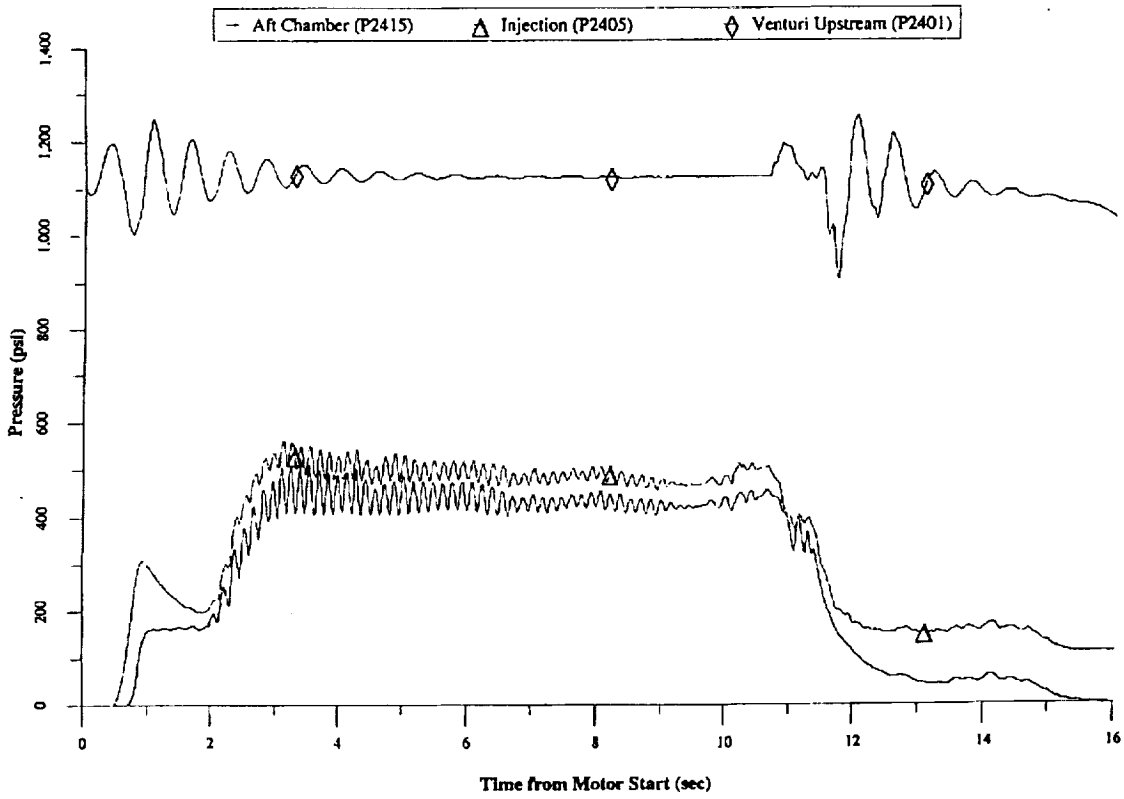

Figure-10: actual system pressures from test-2.

In figure-18, a frequency spectrum of the simulated chamber pressure is presented. There are minor peaks and humps in the spectrum at 0.9 Hz, 1.6 Hz, 2.3 Hz, 2.9 Hz, 3.4 Hz, 4.0 Hz, and 4.7 Hz. The spectral intensity of the peaks and humps seem to decrease with increasing frequency. These peaks and humps seem to be associated with the mean transient of the chamber pressure. These same peaks and humps in the spectral intensity appear in some degree in the spectra of tests-2 and 3.

Test-1 was simulated third. The first attempt at simulating test-1 resulted in non-oscillatory pressures in the combustion chamber and feedsystem downstream of the venturi. Therefore, like tests-2 and 3, the feedline volume downstream of the venturi, between the

valve and injector was increased 14.17 times the actual value. This increase was equivalent to the actual LOX compressibility being 14.17 times the compressibility as it was modeled. This increase resulted in no change in the non-oscillatory pressures in the chamber and in the feedsystem downstream of the venturi. Appearantly, the high-impedance of the injector was effective in damping the oscillations that would have occurred due to a "soft" feedsystem.

RESULTS OF THE TEST-7 SIMULATION:

The actual and simulated test data for test-7 are presented in figures-19 and 20, respectively. Recall that test-7 was performed with a fresh fuel grain, with a LOX flow rate of 20 lbm/sec (9.1 kg/sec), and with the low-impedance JIRAD injector with a pressure drop of 10%. Additionally, test-7 was performed with an orifice immediately upstream of the injector. As in tests-1, 2, and 3, there is a very good qualitative match between the actual and simulated test data. There were minimal yet stable chamber pressure oscillations throughout the test.

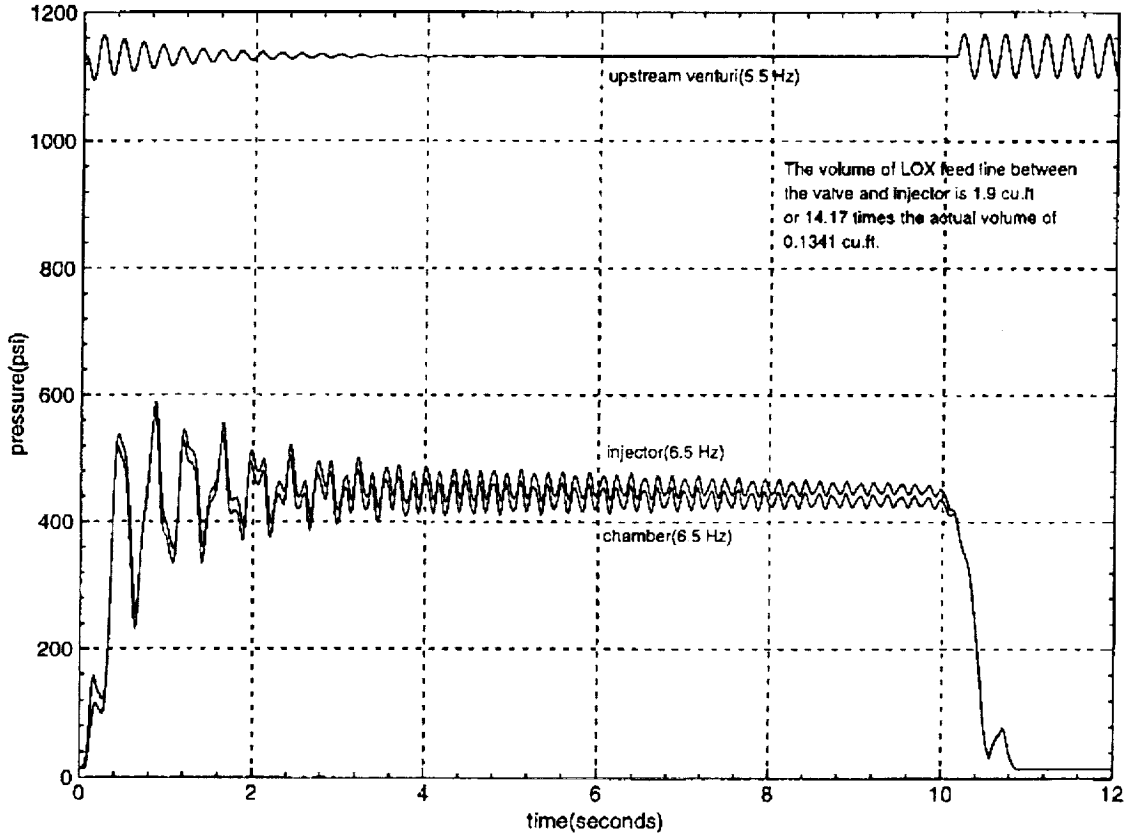

Figure-11: simulated system pressures for test-2.

In figure-21, a frequency spectrum of the simulated chamber pressure is presented. There are minor peaks and humps in the spectrum at 1.4 Hz, 2.3 Hz, and 3.3 Hz. The spectral intensity of the peaks and humps seem to decrease with increasing frequency. These peaks and humps seem to be associated with the mean transient of the chamber pressure. Some of these same peaks and humps in the spectral intensity appear in some degree in the spectra of tests-1, 2, and 3.

Test-7 was simulated last. The first attempt at simulating test-7 resulted in non-oscillatory pressures in the combustion chamber and feedsystem downstream of the venturi.

Therefore, like tests-1, 2 and 3, the feedline volume downstream of the venturi, between the valve and injector was increased 14.17 times the actual value. This increase was equivalent to the actual LOX compressibility being 14.17 times the compressibility as it was modeled. This increase resulted in no change in the non-oscillatory pressures in the chamber and in the feedsystem downstream of the venturi. Appearantly, the orifice increased the effective impedance of the low-impedance injector and was effective in damping the oscillations that would have occurred due to a "soft" feedsystem.

SUMMARY AND CONCLUSIONS:

Agreement between the results of the Matrix-x transient model and the actual test data was very good. This agreement between simulated and actual test data indicated that the non-acoustic combustion instability in the hybrid motor was due to two causes. The first cause was a LOX feed system of excessive capacitance or insufficient stiffness. Capacitance was defined the product of feedline volume and liquid compressibility. Stiffness was defined as the reciprical of capacitance. Modeling a portion of feedline with a volume 14.17 times the actual volume was the same as modeling the actual compressibility as 14.7 times the compressibility as represented in the model. The large compressibility in this portion of feedline suggests the presence of trapped gaseous oxygen (GOX). The portion of feedline in question is between the valve and injector. The second cause was the JIRAD LOX injector that had an impedance or pressure drop that was insufficient to provide damping against the feed system oscillations. However, the LSSRCS LOX injector had sufficient impedance to damp the feed system oscillations. Also, it was discovered that testing with a new grain of solid fuel sustained the combustion instability. However, testing with a used grain of solid fuel caused the combustion instability to gradually decay.

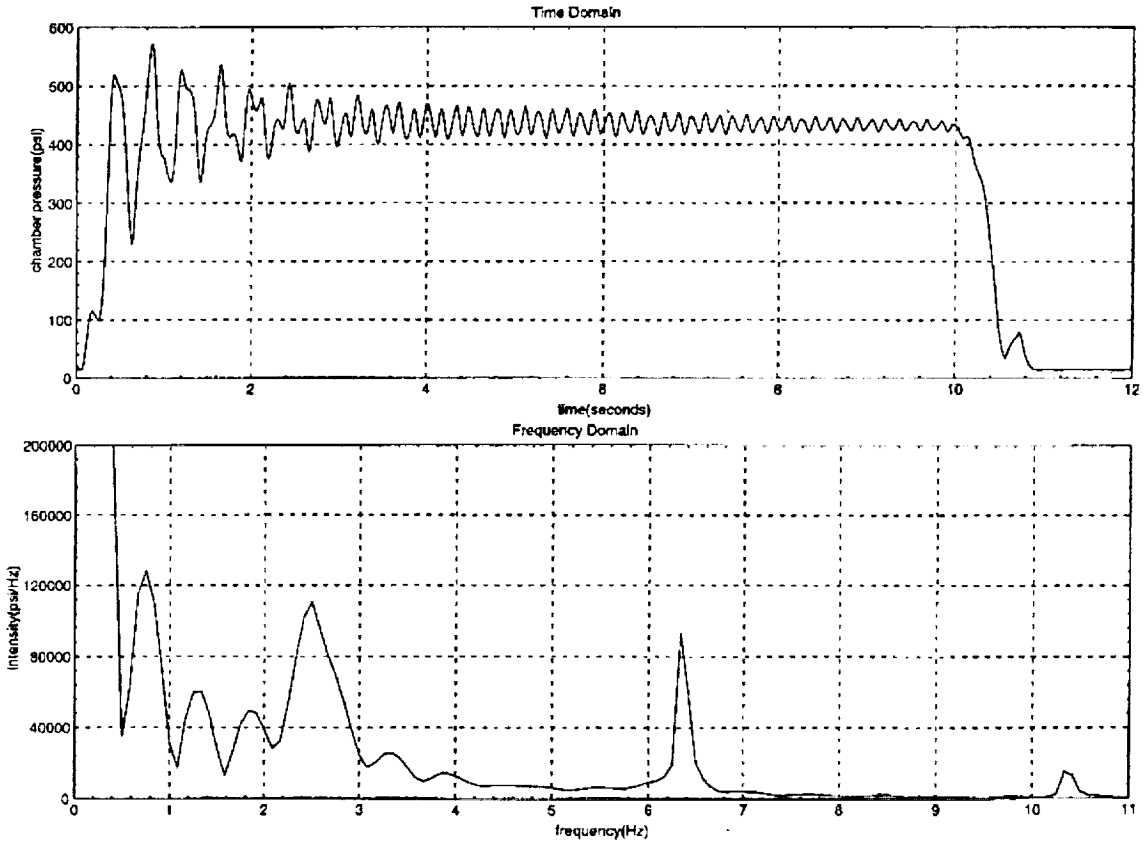

Figure-12: simulated chamber pressure and frequency spectrum for test-2.

In frequency spectrum of the simulated chamber pressure, there were minor peaks and humps in the spectrum at 1.4 Hz, 2.3 Hz, and 3.3 Hz in the case of test-7. In the case of test-1, not only were there minor peaks and humps appearing at frequencies similar to those of test-7, but there were also minor peaks and humps at 0.9 Hz, 2.9 Hz, 4.0 Hz, and 4.7 Hz. The magnitude of the spectral intensity of the peaks and humps seem to decrease with increasing frequency. The peak at 2.3 Hz probably corresponded to the "fill/flush" frequency. Since tests-1 and 7 were stable, these peaks and humps seem to be associated with the mean transient of the chamber pressure.

Also, in the frequency spectrum of the simulated chamber pressure, there were peaks in the spectrum at 2.5 Hz, 6.4 Hz, and 10.4 Hz for tests-2 and 3. The peak at 2.5 Hz was primary in spectral intensity in test-2, secondary in test-3, and corresponded to the "fill/flush" frequency. The peak at 6.4 Hz was slightly secondary in spectral intensity in test-2, dramatically dominant in test-3, and corresponded to the non-acoustic combustion instability associated with the LOX feedline between the valve and the injector. The peak at 10.4 Hz was a distant third in spectral intensity and did not corresponds to any known cause. Since tests-2 and 3 were unstable, the peaks at 6.4 Hz seemed to be associated with the large amplitude oscillations in chamber pressure.

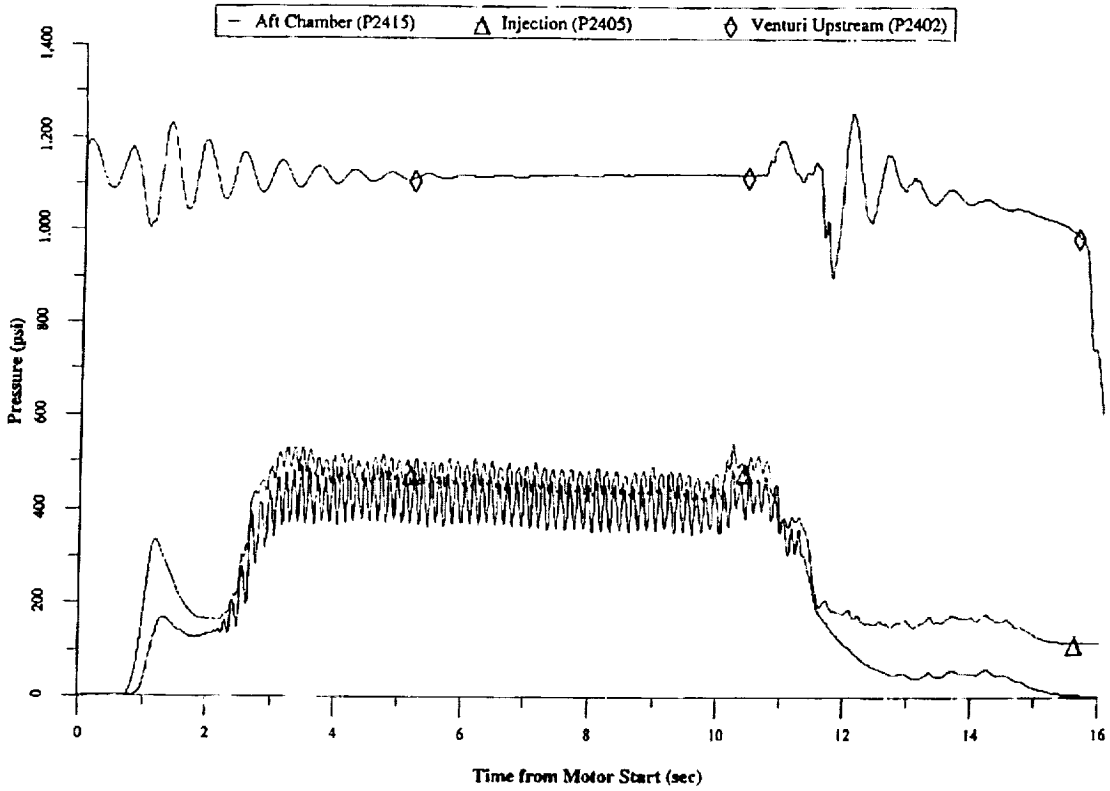

Figure-13: actual system pressures from test-3.

REFERENCES:

1) "Hybrid Rocket Instability", B. E. Greiner and R. A. Frederick, final report: Thiokol Contract PO1175, Proposal 92-444 to the University of Alabama-Huntsville, 1992.

2) "HPTLVB (Hybrid Propulsion Technology for Launch Vehicle Boosters) Motor Testing Final Report", CD-ROM, Contract NAS8-39942, 1996.

3) "Nonacoustic Feed System Coupled Combustion Instability in Hybrid Rocket Motors", T. A. Boardman, D. K. Hawkins, S. R. Wassom, and S. E. Claflin, a presentation at the Hybrid Rocket Technical Committee Combustion Stability Workshop, 31st AIAA/ASME/SAE/ASEE Joint Propulsion Conference and Exhibit, 1995.

4) "Hybrid Propulsion Technology for Launch Vehicle Boosters: A Program Status Update", AIAA 95-2688, R. L. Carpenter, T. A. Boardman, S. E. Claflin, and R. J. Harwell, 1995.

5) Private Communication with Charles L. Martin, Solid and Hybrid Rocket Motor Ballistician, NASA/Marshall Space Flight Center, July, 1999.

6) "An Evaluation of Scaling Effects for Hybrid Rocket Motors", AIAA 91-2517, P. N. Estey, D. Altman, and J. S. McFarlane, 1991.

7) "Liquid Propellant Rocket Combustion Instability", NASA SP-194, editors: D. T. Harrje and F. H. Reardon, 1972, page-108.

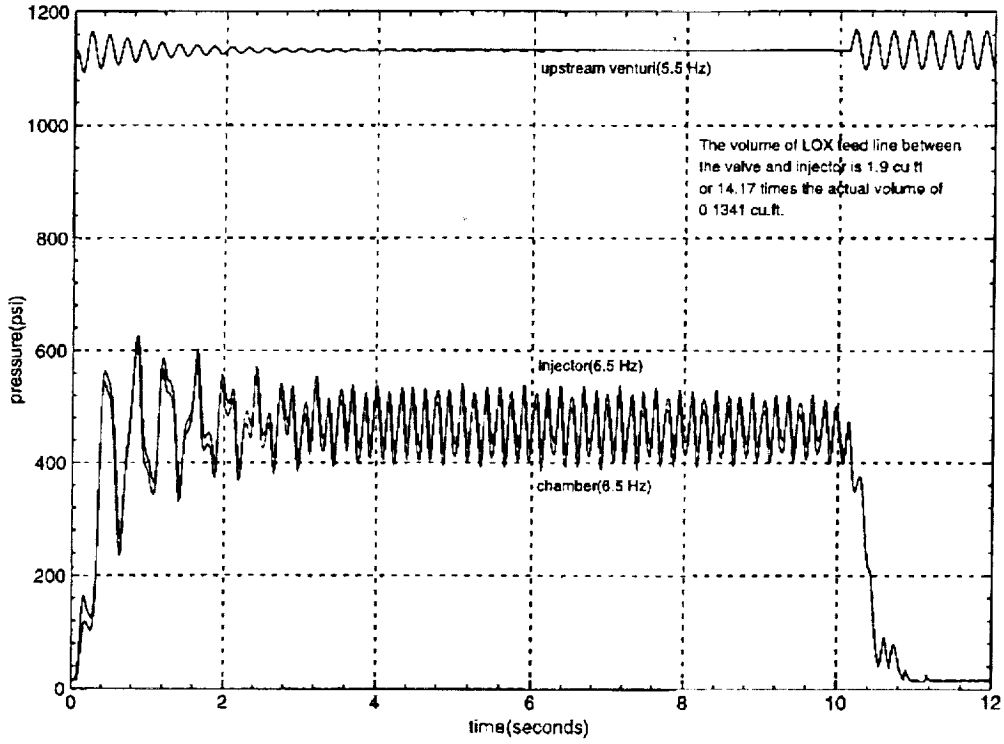

Figure-14: simulated system pressures for test-3.

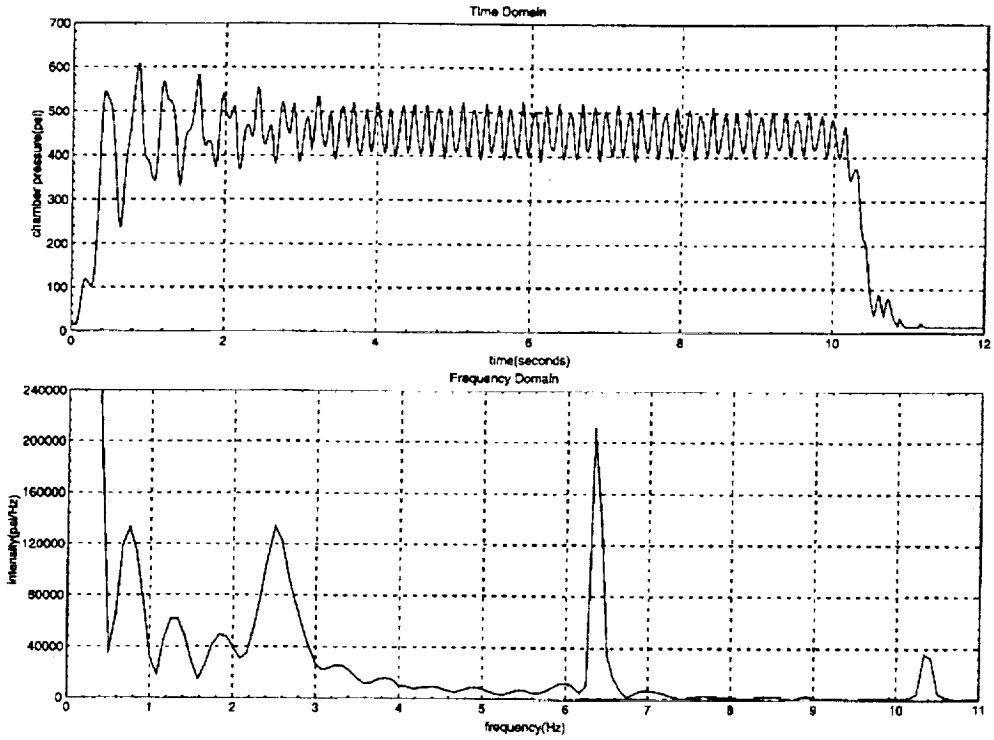

Figure-15: simulated chamber pressure and frequency spectrum for test-3.

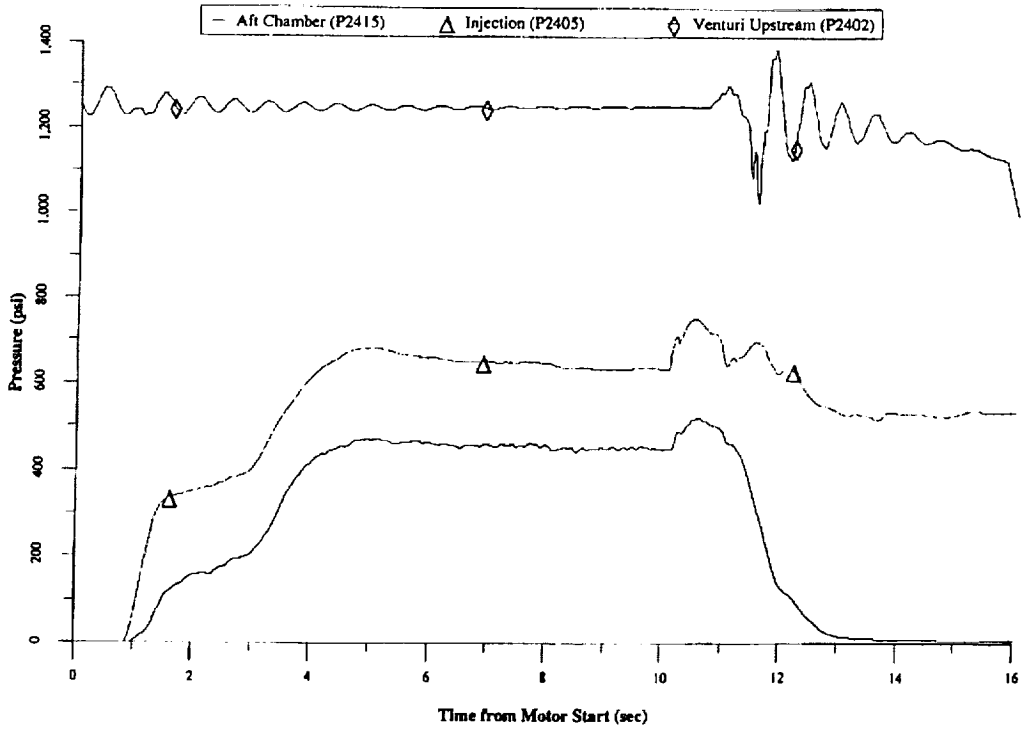

Figure-16: actual system pressures from test-1.

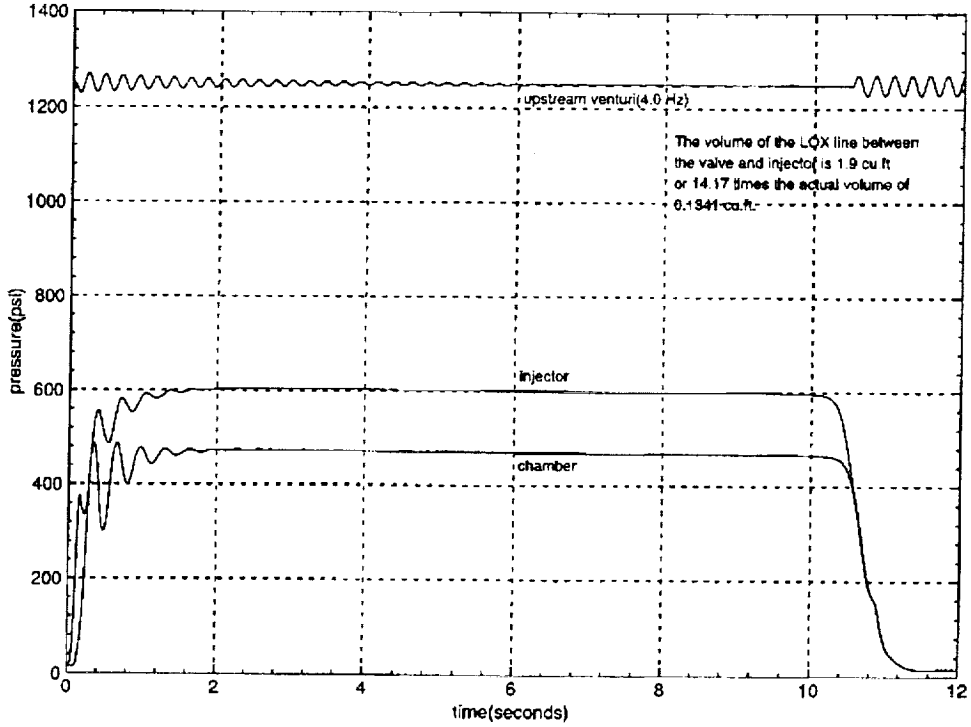

Figure-17: simulated system pressures for test-1.

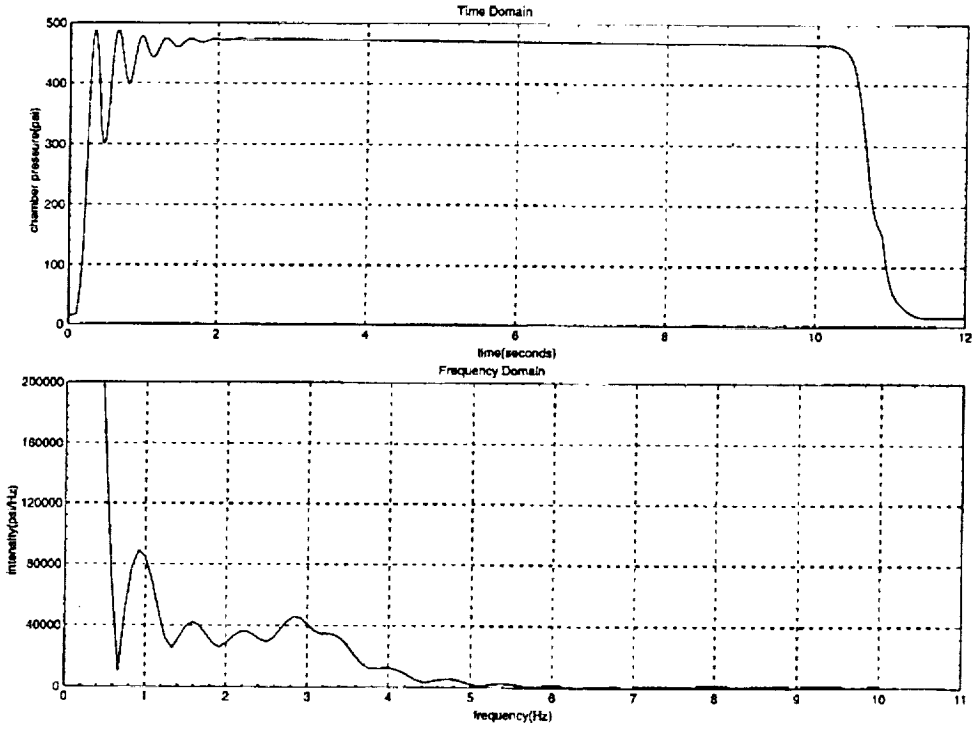

Figure-18: simulated chamber pressure and frequency spectrum for test-1.

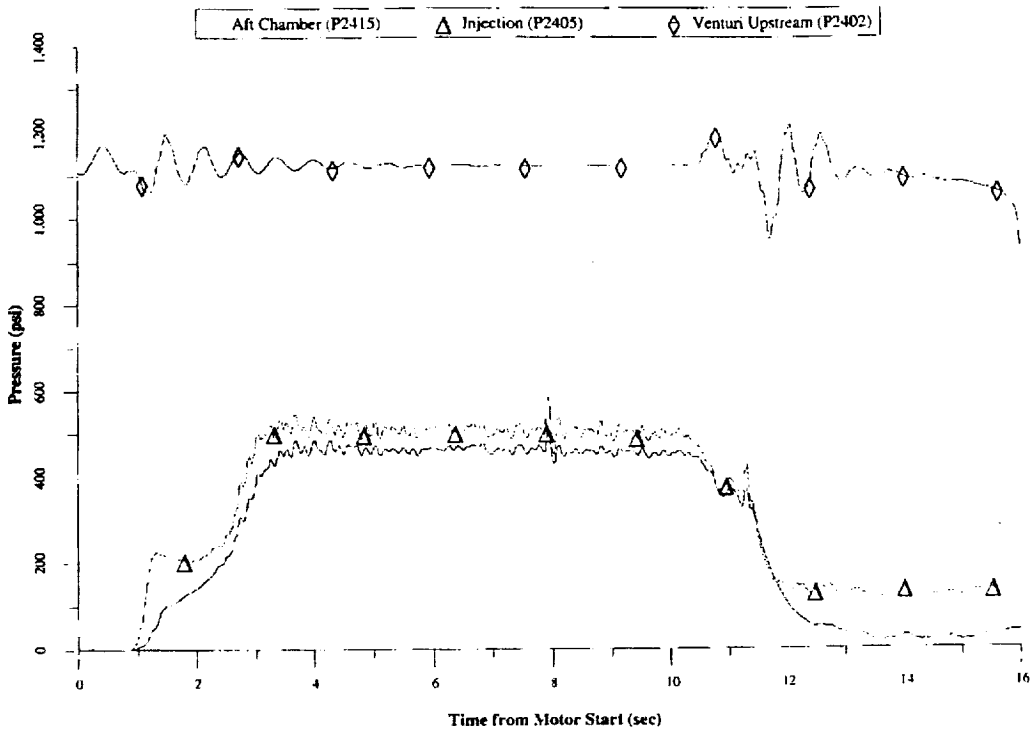

Figure-19: actual system pressures from test-7.

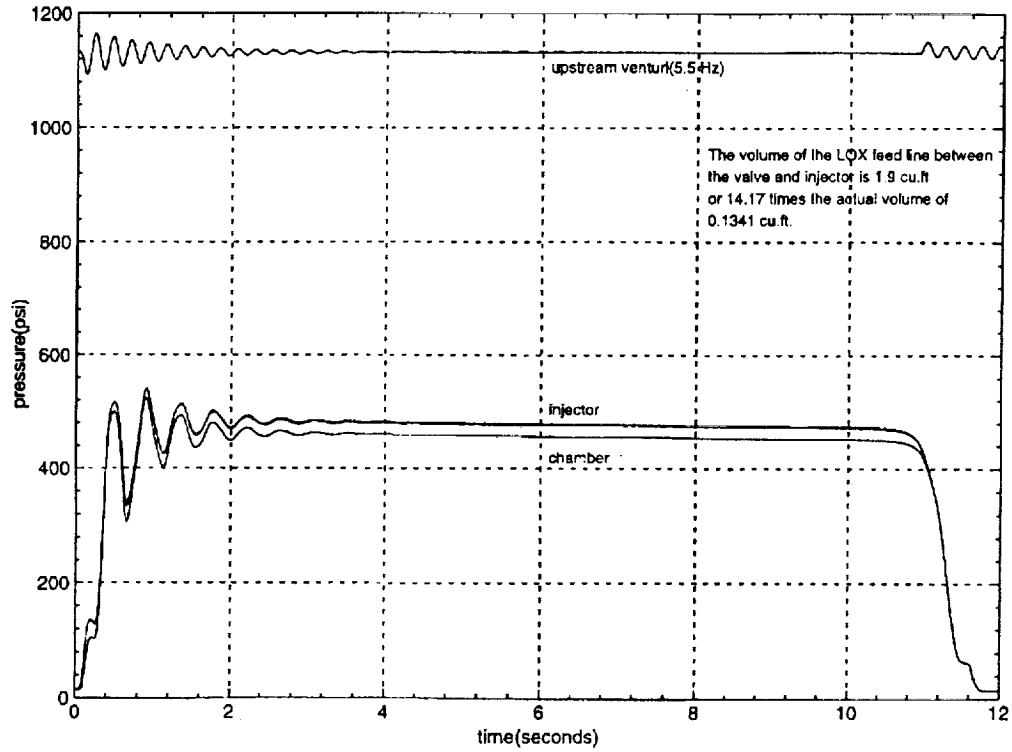

Figure-20: simulated system pressures for test-7.

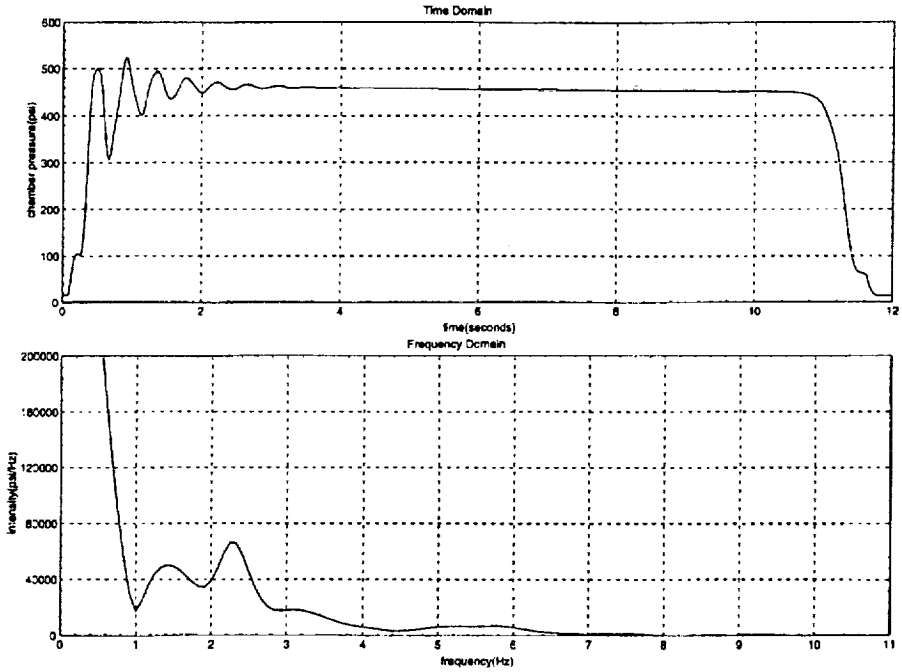

Figure-21: simulated chamber pressure and frequency spectrum for test-7.